

See discussions, stats, and author profiles for this publication at: <https://www.researchgate.net/publication/7900847>

Simultaneous Conductivity and Viscosity Measurements as a Technique To Track Emulsion Inversion by the Phase-Inversion-Temperature Method

ARTICLE in LANGMUIR · APRIL 2004

Impact Factor: 4.46 · DOI: 10.1021/la035334r · Source: PubMed

CITATIONS

55

READS

86

5 AUTHORS, INCLUDING:



[Joachim Allouche](#)

Université de Pau et des Pays de l'Adour

22 PUBLICATIONS 480 CITATIONS

[SEE PROFILE](#)



[Eric Tyrode](#)

KTH Royal Institute of Technology

42 PUBLICATIONS 990 CITATIONS

[SEE PROFILE](#)



[Véronique Sadtler](#)

Ecole Nationale Supérieure Des Industries Ch...

36 PUBLICATIONS 458 CITATIONS

[SEE PROFILE](#)



[Jean-Louis Salager](#)

University of the Andes (Venezuela)

197 PUBLICATIONS 3,723 CITATIONS

[SEE PROFILE](#)

Simultaneous Conductivity and Viscosity Measurements as a Technique To Track Emulsion Inversion by the Phase-Inversion-Temperature Method

Joachim Allouche,[†] Eric Tyrode,[‡] Véronique Sadtler,[†] Lionel Choplin,[†] and Jean-Louis Salager^{*,‡}

Centre de Génie Chimique des Milieux Rhéologiquement Complexes (GEMICO), Ecole Nationale Supérieure des Industries Chimiques (ENSIC), Nancy, France, and Laboratorio FIRP, Ingeniería Química, Universidad de Los Andes, Avenida Don Tulio Febres, Mérida 5101, Venezuela

Received July 22, 2003. In Final Form: December 1, 2003

Two kinds of transitions can occur when an emulsified water–oil–ethoxylated nonionic surfactant system is cooled under constant stirring. At a water–oil ratio close to unity, a transitional inversion takes place from a water-in-oil (W/O) to an oil-in-water (O/W) morphology according to the so-called phase-inversion-temperature method. At a high water content, a multiple w/O/W emulsion changes to a simple O/W emulsion. The continuous monitoring of both the emulsion conductivity and viscosity allows the identification of several phenomena that take place during the temperature decrease. In all cases, a viscosity maximum is found on each side of the three-phase behavior temperature interval and correlates with the attainment of extremely fine emulsions, where the best compromise between a low-tension and a not-too-unstable emulsion is reached. The studied system contains Polysorbate 85, a light alkane cut oil, and a sodium chloride brine. All transitions are interpreted in the framework of the formulation–composition bidimensional map.

Introduction

The phase behavior of water–oil–surfactant systems essentially depends on the relative affinity of the surfactant for the oil and water phases, and a swap in surfactant affinity is directly associated to the phase behavior transition.^{1–4} According to pioneering work by Winsor,^{5,6} when the interactions between surfactant and water (respectively oil) are dominant, the phase behavior of the system is the so-called Winsor I type, noted WI (respectively Winsor II type, denoted WII), and an aqueous (respectively oily) microemulsion is in equilibrium with an excess predominantly oily (respectively aqueous) phase. Between these two-phase behavior cases, a three-phase behavior (WIII) prevails, in which a bicontinuous microemulsion is in equilibrium with aqueous and oily excess phases. Such behavior depends on several physicochemical parameters, whose effects can be gathered in a single formulation variable, so-called the hydrophilic lipophilic deviation (HLD). The HLD is some kind of system hydrophilic lipophilic balance; that is, it is a quantitative measurement of the deviation from a balanced formulation, in terms of all formulation variables. This generalized formulation variable has been shown to be related to the partition coefficient of the surfactant between the two phases^{7,8} and to the difference of chemical potential of the

surfactant in the aqueous and oleic phases, so-called “surfactant-affinity difference”.^{9,10}

It is essentially equivalent to an empirical expression found 25 years ago for the attainment of three-phase behavior, which is as follows for nonionic systems:¹¹

$$\text{HLD} = \alpha - \text{EON} - k\text{ACN} + bS + \Phi(A) + c_T(T - T_{\text{ref}}) \quad (1)$$

where α is a characteristic parameter of the hydrophobic part of the surfactant; EON is the number of ethylene oxide groups per surfactant molecule; ACN is the number of carbon atoms in the alkane molecule (or equivalent); S is the salinity of the aqueous phase in wt % NaCl (or equivalent); $\Phi(A)$ is function of the alcohol type and concentration; T is the temperature (°C); T_{ref} is generally taken at 25 °C; and k , b , and c_T are constants, characteristic of the surfactant type and electrolyte.

The correspondence is such that $\text{HLD} < 0$ (respectively $\text{HLD} > 0$) corresponds to WI (respectively WII) phase behavior and $\text{HLD} = 0$ corresponds to so-called optimum formulation for three-phase behavior (WIII).

The high value of the temperature coefficient c_T for the ethoxylated nonionic system, for example, typically four times larger than for anionic systems,^{8,12,13} indicates that

* Corresponding author. E-mail: salager@ula.ve.

[†] Ecole Nationale Supérieure des Industries Chimiques.

[‡] Universidad de Los Andes.

(1) Bourrel, M.; Graciaa, A.; Schechter, R. S.; Wade, W. H. *J. Colloid Interface Sci.* **1979**, *72*, 161.

(2) Vinatieri, J. E. *Soc. Pet. Eng. J.* **1980**, *20*, 402.

(3) Salager, J. L.; Quintero, L.; Ramos, E.; Andérez, J. M. *J. Colloid Interface Sci.* **1980**, *77*, 287.

(4) Milos, F. S.; Wasan, D. T. *Colloids Surf., A* **1982**, *4*, 91.

(5) Winsor, P. A. *Solvent Properties of Amphiphilic Compounds*; Butterworth: London, 1954.

(6) Bourrel, M.; Schechter, R. S. *Microemulsion and Related Systems*; Marcel Dekker: New York, 1988.

(7) Salager, J. L.; Marquez, N.; Graciaa, A.; Lachaise, J. *Langmuir* **2000**, *16*, 5534.

(8) Salager, J. L.; Antón, R. E.; Andérez, J. M.; Aubry, J. M. *Techniques de l'Ingénieur*; Paper no. 157; 2001; Vol. J2.

(9) Salager, J. L. In *Handbook of detergent – Part A: Properties*; Broze, G., Ed.; Marcel Dekker: New York, 1999; p 253.

(10) Salager, J. L. In *Pharmaceutical Emulsions and Suspensions*; Nielloud, F.; Marti-Mestres, G., Eds.; Marcel Dekker: New York, 2000; Chapter 2, p 19.

(11) Bourrel, M.; Salager, J. L.; Schechter, R. S.; Wade, W. H. *J. Colloid Interface Sci.* **1980**, *75*, 451.

(12) Salager, J. L.; Morgan, J.; Schechter, R. S.; Wade, W. H.; Vasquez, E. *Soc. Pet. Eng. J.* **1979**, *19*, 107–115.

(13) Antón, R. E.; Garcés, N.; Yajure, A. *J. Dispersion Sci. Technol.* **1997**, *18*, 539–555.

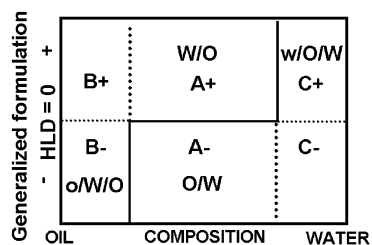


Figure 1. Formulation-composition bidimensional map.

temperature has a strong effect on the formulation of these kinds of systems, which is why temperature is often selected as the scanning variable to induce a change in formulation with ethoxylated nonionic surfactants and the associated emulsion inversion.^{14–16} However, it is worth pointing out that such a change can be produced by any of the variables or combination of variables listed in eq 1 HLD expression.^{17,18}

The emulsion morphology also depends on the water-to-oil ratio (WOR), and this is clearly indicated in the bidimensional map introduced 20 years ago to describe the combined effect of formulation (including temperature and pH) and WOR¹⁹ and currently used in many instances (Figure 1).^{18,20–24}

The bold line is the inversion frontier, that is, the boundary that separates the regions where oil external (W/O) and water external (O/W) emulsions are found in this map when an equilibrated surfactant-oil-water system, having the corresponding formulation and water/oil composition, is stirred. This line is essentially composed of a central horizontal branch and two lateral vertical branches. The central region is labeled “A” with a “+” (respectively “-”) superscript to indicate that the region is located above, at HLD > 0 (respectively below at HLD < 0), the optimum or neutral tendency formulation line (HLD = 0).

The lateral branches of the inversion line essentially correspond to a constant oil/water composition, typically located at 30 and 70% water. The left part region is labeled “B” and the right part “C”, both with the same superscript symbol as in the central region. The B⁺ region is found to be phenomenologically identical to the A⁺ region, and there is no real boundary between them but a simple change in the WOR. It is the same for the A⁻ and C⁻ regions. All these A⁻C⁻ and A⁺B⁺ regions are called normal regions because the emulsion type corresponds to the curvature that is favored by the physicochemical formulation effect, a situation that is often referred to as Bancroft’s rule.^{25,26} On the contrary, the C⁺ and B⁻ regions are so-called abnormal¹⁹ because the external phase is not the one that is expected by applying Bancroft’s rule. Instead, it is the

external phase favored by Ostwald’s rule; that is, it is the phase existing in a higher volume in the system.^{27,28}

In these abnormal regions, multiple emulsions are often produced by simple stirring.¹⁹ They are of the o/W/O type in B⁻ and w/O/W type in C⁺, where the lower case letter indicates the most internal phase, that is, the droplets inside the drops. It can be said that the spontaneous occurrence of a multiple emulsion is a way for the system to satisfy conflicting inclinations, as far as interface curvature is concerned. The most interior or “inner” emulsion is of the type imposed by the formulation, for example, w/O in the C⁺ region, whereas the external or “outer” one is the type demanded by the water/oil composition, for example, O/W in the C⁺ region.

The combined effects of formulation and water/oil composition allow the targeting and changing of the emulsion type according to an emulsification protocol. In particular, the variation of formulation can provide two kinds of dynamics transitions, at fixed composition and under constant stirring.

The first one, which is the transitional inversion of a W/O into an O/W emulsion, is associated to the crossing of the inversion line between from A⁺ to A⁻ normal regions at intermediate WOR. It was reported a few years ago²⁹ that the drop size in the vicinity of optimal formulation exhibits a complex variation as the result of a dynamic equilibrium between two strong and opposite effects. As the HLD = 0 formulation is approached from both sides, the interfacial tension decrease favors the breaking process and, thus, tends to produce a smaller drop size and an associated higher viscosity. However, the emulsion stability decreases strongly as well, and drops are likely to coalesce instantly upon contact very near HLD = 0, which favors the opposite trend, that is, the attainment of a larger drop size and a reduction in emulsion viscosity. The first effect dominates relatively far from HLD = 0, whereas the latter prevails closer to it. This results in a complex variation of the drop size, which exhibits two minima, one on each side of optimal formulation. As a consequence, the viscosity would exhibit the two corresponding maxima, as indicated in Figure 2.

The general phenomenology found for the effect of HLD on the drop size applies over a wide range of WOR and with all formulation variables,³⁰ in particular to describe the effect of temperature.²⁹ When a continuous change of temperature is carried out under constant stirring, the emulsion inversion takes place at the so-called phase inversion temperature (PIT),³¹ which essentially corresponds to HLD = 0 in a temperature scan, unless very atypical conditions are met.³²

As a consequence of the previously discussed variation of the drop size, there is a particularly favorable situation to produce a fine drop O/W emulsion at a temperature just below the PIT, as noted a long time ago³³ and developed in detail in the past decade^{34,35} to take advantage of the

(14) Shinoda, K.; Arai, H. *J. Phys. Chem.* **1964**, *68*, 3485–3490.

(15) Kahlweit, K. *J. Colloid Interface Sci.* **1982**, *90*, 197.

(16) Kahlweit, M.; Lessner, E.; Strey, R. *J. Phys. Chem.* **1984**, *88*, 1937.

(17) Salager, J. L.; Márquez, L.; Peña, A.; Rondon, M. J.; Silva, F.; Tyrode, E. *Ind. Eng. Chem. Res.* **2000**, *39*, 2665.

(18) Miller, D. J.; Henning, T.; Grünbein, W. *Colloids Surf., A* **2001**, *183–185*, 681.

(19) Salager, J. L.; Miñana-Pérez, M.; Pérez-Sánchez, M.; Ramirez-Gouveia, M.; Rojas, C. *J. Dispersion Sci. Technol.* **1983**, *4*, 313.

(20) Davis, H. T. *Colloids Surf., A* **1994**, *91*, 9.

(21) Dickinson, E. *Annual Reports C, The Royal Soc. Chem.* **1986**, *31–58*.

(22) Brooks, B. W.; Richmond, H. N. *Colloids Surf., A* **1991**, *58*, 131.

(23) Brooks, B. W.; Richmond, H. N. *Chem. Eng. Sci.* **1994**, *49*, 1053–1064.

(24) Méndez, Z.; Antón, R. E.; Salager, J. L. *J. Dispersion Sci. Technol.* **1999**, *20*, 883.

(25) Bancroft, W. D. *J. Phys. Chem.* **1913**, *17*, 501.

(26) Bancroft, W. D. *J. Phys. Chem.* **1915**, *19*, 275.

(27) Ostwald, W. *Kolloid-Z.* **1910**, *6*, 103.

(28) Ostwald, W. *Kolloid-Z.* **1910**, *7*, 64.

(29) Salager, J. L.; Pérez-Sánchez, M.; Garcia, Y. *Colloid Polym. Sci.* **1996**, *274*, 81.

(30) Pérez, M.; Zambrano, N.; Ramirez, M.; Tyrode, E.; Salager, J. L. *J. Dispersion Sci. Technol.* **2002**, *23*, 55–63.

(31) Shinoda, K.; Kunieda, H. In *Encyclopedia of Emulsion Technology*; Becher, P., Ed.; Marcel Dekker: New York, 1985; Vol. 1, Chapter 5.

(32) Antón, R. E.; Castillo, P.; Salager, J. L. *J. Dispersion Sci. Technol.* **1986**, *7*, 319–329.

(33) Shinoda, K.; Saito, H. *J. Colloid Interface Sci.* **1969**, *30*, 258.

(34) Förster, T.; Rybinsky, W. V.; Tesmann, H.; Wadle, A. *Int. J. Cosmet. Sci.* **1994**, *16*, 84.

(35) Wadle, A.; Tesmann, H.; Leonard, M.; Förster, T. *Surf. Sci. Series* **1997**, *68*, 207.

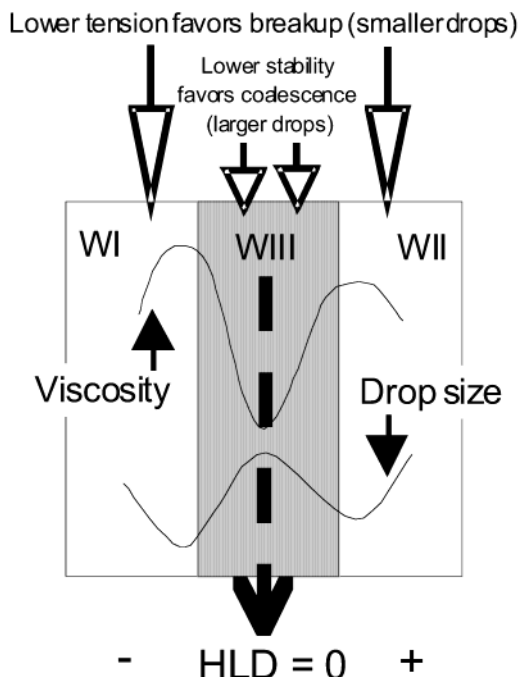


Figure 2. Maximum in viscosity and minimum in drop size on each side of the three-phase behavior interval.

combination of low interfacial tension and not-too-unstable droplets. Generally, the stabilization of the fine droplets is enhanced either by a rapid cooling of the emulsion to shift the HLD far away from the unstable region or by the deposition of a liquid crystal layer, which avoids the coalescence of the formed droplets as it normally happens near the PIT.^{33,36–41}

The surfactant-affinity change during the emulsion transitional inversion is also likely to result in complex morphologies such as multiple emulsions. For instance, during the inversion of a W/O emulsion into an O/W one, multiple emulsions of the o/W/O or w/O/W type have been found to occur by the inclusion of the continuous phase into the dispersed phase.^{42,43} Inclusion is an essential element in the mechanism of the inversion process, and it can result in more complex morphologies in the presence of a microemulsion (M) third phase such as M/O/M or (W+O)/M.^{44–48}

The second transition to be dealt with here, which is associated to a very high water content, is substantially different from the previous one. The initial emulsion is a multiple w/O/W emulsion imposed by the $HLD > 0$ and high-water-content conditions prevailing in the map C⁺ region, as discussed before. Hence, reducing the temper-

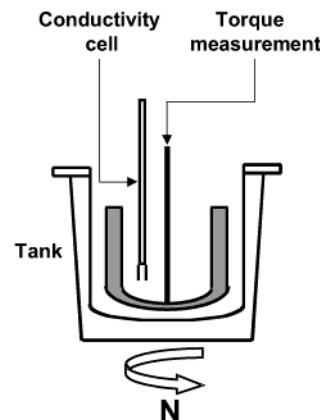


Figure 3. “Rheomixer” device.

ature does not induce the crossing of the inversion line but results in a transition from C⁺ to C[−] and the corresponding change from a w/O/W multiple emulsion into a simple O/W one.

This paper aims at returning more information on the involved mechanisms by the in situ tracking of the viscosity and conductivity concomitant changes during these dynamic transitions.

Experimental Section

Materials. The oily phase contains kerosene with a small amount of 2-propanol (Fluka Chemika, France). 2-Propanol (2 vol % with respect to the total system volume) is known to inhibit the formation of mesophases and liquid crystals and to speed the drop breakup and, thus, virtually eliminate the hysteresis that can eventually take place near the PIT.⁴⁹ Moreover, its influence on the HLD is essentially insignificant [$\Phi(A) \approx +0.05$, that is, of the same order as a 1 °C change in temperature]. Purified water (Milli-Q Millipore) is used to prepare the NaCl (purity > 99.5%, Merck) brine at 1 g of NaCl per 100 mL of water phase, essentially 1 wt %. The used surfactant is a polyethoxylated sorbitan trioleate (Tween 85, HLB = 11) with an average of 20 ethylene oxide groups per surfactant molecule (Fluka Chemika). The concentration of the surfactant is 4.5 g per 100 mL of system, which is close to 4.5 wt % (as indicated in the figure).

Methods. Each experience is realized for three different compositions corresponding to high, low, and intermediate water contents (FW = fraction of water): FW = 0.35, that is, 35 vol % water and 65 vol % oil; FW = 0.50, that is, 50 vol % water and 50 vol % oil; and FW = 0.70, that is, 70 vol % water and 30 vol % oil.

After the samples are prepared, they are placed in a closed vessel and left to equilibrate for 24 h in a constant temperature enclosure at 50 °C, which is the initial temperature in all experiments.

The emulsification process and temperature transition experiment is carried out in a “rheomixer” device that consists of a jacketed vessel and an impeller connected to a RFS II rheometer (Rheometric Scientific, U.S.A.). The vessel is located on a rotating turntable, whereas the impeller and the conductivity cell are in a fixed position, as indicated in Figure 3. As a consequence, the impeller is in relative motion with respect to the content of the vessel, and the torque produced by this motion can be detected by the rheometer. In the present case, the impeller is a U-type anchor, but other geometries are also used, for example, helicoidal ribbon, depending of the viscosity of the fluids. The regulation and change of temperature is ensured by circulation of a heat-conveying fluid from a thermostatic bath (Huber, Germany) to a double-walled device fixed around the vessel.

A Couette analogy method has been recently reported to analyze the torque–rotational speed data of this kind of device, to extract “absolute” viscosity–shear rate data similar to what is attained in a conventional geometry rheometer.⁵⁰

(36) Friberg, S.; Jansson, P. O. *J. Colloid Interface Sci.* **1976**, *55*, 614–623.

(37) Sagitani, H. *J. Dispersion Sci. Technol.* **1988**, *9*, 115.

(38) Suzuki, T.; Takei, H.; Yamazaki, S. *J. Colloid Interface Sci.* **1989**, *129*, 491.

(39) Rouvière, J.; Razakarison, J. L.; Marignan, J.; Brun, B. *J. Colloid Interface Sci.* **1989**, *133*, 293.

(40) Izquierdo, P.; Esquena, J.; Tadros, Th.; Dederen, C.; Garcia, M. J.; Azemar, N.; Solans, C. *Langmuir* **2002**, *18*, 26.

(41) Forgiarini, A.; Esquena, J.; Gonzalez, C.; Solans, C. *Langmuir* **2001**, *17*, 2076.

(42) Pacek, A. W.; Moore, I. P. T.; Nienow, W.; Calabrese, R. V. *AIChE J.* **1994**, *40*, 190.

(43) Groeneweg, F.; Agterof, W. G.; Jaeger, P.; Janssen, J. J. M.; Wieringa, J. A.; Klahn, J. K. *Trans. IChemE* **1998**, *76*, 55.

(44) Lim, K. H.; Smith, D. H. *J. Colloid Interface Sci.* **1991**, *142*, 278.

(45) Smith, D. H.; Johnson, G. K.; Wang, Y. H.; Lim, K. H. *Langmuir* **1994**, *10*, 2516.

(46) Kumar, S. *Chem. Eng. Sci.* **1996**, *51*, 831.

(47) Lee, J. M.; Lim, K. H.; Smith, D. H. *Langmuir* **2002**, *18*, 7334.

(48) Lee, J. M.; Lim, K. H. *J. Ind. Eng. Chem.* **2002**, *8*, 89.

(49) Márquez, L.; Graciaa, A.; Lachaise, J.; Salager, J. L.; Zambrano, N. *Polym. Int.* **2003**, *52*, 590–593.

The Couette analogy allows the determination of the radius R_i of an equivalent Couette inner cylinder, having the same height L as the impeller, and resulting in the same torque C for the same rotational speed N , in a cylinder with the same radius R_e as the actual vessel. Solving the equations of change in this virtual Couette geometry, and assuming steady-state, laminar-regime, and isothermal conditions for a power-law fluid behavior represented by

$$\eta = k\dot{\gamma}^{n-1} \quad (2)$$

where k and n are the consistency and the flow index, respectively, R_i can be calculated to be

$$R_i = \frac{R_e}{\left[1 + \frac{4\pi N}{n} \left(\frac{2\pi k L R_e^2}{C} \right)^{1/n} \right]^{n/2}} \quad (3)$$

It is worth remarking that, for a given set of (N, C) values, R_i is a weak function of n . Therefore, the determination of R_i can be carried out for the particular case of a Newtonian fluid ($n = 1$) of known viscosity. Once R_i has been determined in the virtual Couette geometry, the shear stress and the shear rate profiles can be calculated, as well as the viscosity at a given position in the virtual gap. In this case, the shear stress is given by

$$\tau = \frac{C}{2\pi L r^2} \quad (4)$$

and the shear rate, for a power-law fluid, is

$$\dot{\gamma} = \left\{ \frac{4\pi}{n} \left(\frac{R_i}{r} \right)^{2/n} \left[1 - \left(\frac{R_i}{R_e} \right)^{2/n} \right] \right\} N \quad (5)$$

Even for a large $(R_e - R_i)$ virtual gap, it has been found that a specific position in the gap, noted r^* , exists at which the term in braces in eq 5 is essentially independent of the power-law index n , that is, of the fluid rheological behavior. Hence, this r^* value may be calculated in the particular case of $n = 1$, and then both the shear stress and the shear rate can be evaluated at $r = r^*$:

$$\tau_{r^*} = \frac{C}{2\pi L (r^*)^2} \quad (6)$$

and

$$\dot{\gamma}_{r^*} = \frac{4\pi N (R_i/r^*)^2}{1 - (R_i/R_e)^2} \quad (7)$$

The viscosity may be calculated as the ratio $\tau_{r^*}/\dot{\gamma}_{r^*}$, at a corresponding effective shear rate $\dot{\gamma}_{r^*}$.

This method has been tested for several vessel-impeller combinations and for several rheologically complex systems, such as food emulsions like mayonnaise and salad dressing. The experimental results were found to fit fairly well with those obtained using conventional geometries over a wide range of shear rates, within the experimental error estimated to be no more than 5%.^{50–52}

The emulsification is carried out directly in the “rheomixer” at a constant rotational speed of the impeller that corresponds, for the specific geometrical arrangement, to an effective shear rate of 100 s^{-1} , which is attained at 170 rpm for the selected rheomixer configuration. The temperature is first maintained at 50°C until a constant value of viscosity is reached. Then, the temperature is made to decrease monotonically down to 10°C at a 0.05°C/s cooling rate. Because of the small effective volume

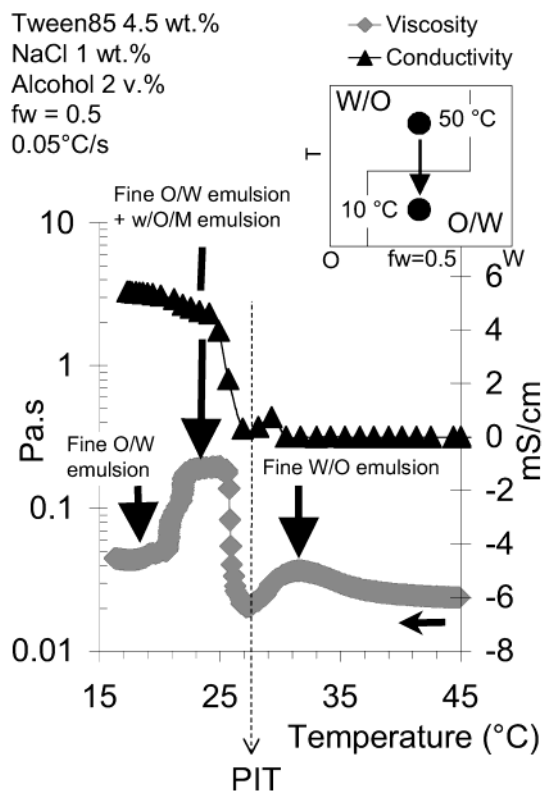


Figure 4. Viscosity (Pa.s) and conductivity (mS/cm) variation as the temperature decreases for FW = 0.5.

of emulsion in the “rheomixer” and because of the continuous homogenization produced by the impeller, the measured temperature is very indicative of the whole emulsion condition ($\pm 0.05^\circ\text{C}$).

Simultaneously to the viscosity and temperature measurements, the conductivity is monitored with a LF340 conductimeter and a Tetracon cell 325 (WTW, Germany), as illustrated in Figure 3. Provided that a relation between the water volume fraction and the theoretical value of the conductivity of a simple O/W emulsion is known, the presence of encapsulated water due to a multiple emulsion morphology can be estimated from a lower than expected conductivity.

The drop size is estimated by withdrawing a small emulsion aliquot with a syringe and then using a Mastersizer Hydro 2000 MU analyzer (Malvern Instruments, U.K.).

Results and Discussion

Transitional Inversions. The first case deals with a system containing equal amounts of oil and water (FW = 0.5). Figure 4 shows the evolution of both the emulsion conductivity and the viscosity while the temperature is monotonically decreased and the system is maintained under constant stirring ($\dot{\gamma} = 100 \text{ s}^{-1}$). The corresponding path on the map during the transitional inversion is represented as an inset in Figure 4 from 50°C (at which $\text{HLD} = +1.3$) to 10°C (at which $\text{HLD} = -1.0$).

The initial W/O emulsion exhibits an essentially zero conductivity from 50°C down to 31°C , at which temperature a first maximum in viscosity is exhibited. This maximum is certainly associated to the occurrence of a drop-size minimum, which is due to the best compromise between a low tension and a quick coalescence rate, as previously discussed.

Just below 31°C , the conductivity increases slightly to 0.8 mS/cm . This change is significant, and it indicates that some morphological change takes place in the system. Dispersibility experiments are carried out by withdrawing

(50) Ait-Kadi, A.; Marchal, P.; Chrissemant, A. S.; Choplin, L.; Bousmina, M. *Can. J. Chem. Eng.* **2002**, *80*, 1166–1174.

(51) Choplin, L.; Marchal, P. *Annu. Trans. Nord. Rheol. Soc.* **1999**, *7*, 5–12.

(52) Choplin, L.; Marchal, P. *Proc. 1st Int. Symp. Food Rheol. Structure*; **1997**, *40*.

a small aliquot and pouring it immediately into oil or water. The instantaneous dispersion occurs in oil, indicating that the outer phase remains the oil. However, the conductivity is much too high for an ordinary W/O emulsion and the appearance of some bicontinuous structure due to the presence of a slightly conductive microemulsion might be the best explanation for this conductivity "bump" around 28 °C. Another explanation could be the presence of large coalescing water drops, which are known to happen just in this location^{53,54} and could cause some conduction through a percolation mechanism, although this is less likely to produce a repeatable and steady peak.

From 27 °C down to 23 °C, the conductivity undergoes a sudden and considerable increase up to 4.5 mS/cm. Dispersibility experiments carried out in this temperature range indicate that the system is instantaneously dispersible in neither water nor oil. We can notice, furthermore, that at 25 °C, the phase behavior of this system is WIII type, that is, a bicontinuous microemulsion in equilibrium with aqueous and oily excess phases. Because the volume ratio of the microemulsion is around 30–35% with respect to the total volume, we can suppose that the "external phase" of the emulsified system is very probably a microemulsion.⁴⁷

The inner water phase at 27 °C starts to move toward the external phase, and the conductivity increases accordingly. Concomitantly, the system viscosity increases significantly and reaches a maximum around 24 °C. This should correspond to a complex "mixture" of fine O/W emulsions with a multiple w/O/M emulsion. It is worth noting that this corresponds to the minimum drop size located below the PIT. However, the viscosity maximum is much higher than the one located slightly above the PIT, a hint that the external phase content is lower, hence the hypothesis of a multiple emulsion, which is corroborated by the insufficient conductivity.

From 23 °C up to 20 °C, the conductivity continues to increase slightly up to a plateau value around 5.5 mS/cm, which corresponds to a simple O/W morphology, while the viscosity decreases sharply. Dispersibility experiments indicate that the emulsion instantaneously disperses into water at 23 °C and below. This means that from 23 °C to 20 °C the system progressively becomes a simple O/W emulsion. It is worth noting, however, that it is a fine emulsion according both to the drop-size estimation and to its relatively high viscosity.

Because of experimental limitations, it was not possible to continuously measure the drop size by laser light scattering. On the other hand, the extreme instability of emulsions near optimum formulation results in quick alteration while a sample is taken and diluted. However and despite the inherent inaccuracies of the sampling process, it is possible to estimate whether the drop size becomes larger or smaller. Finally, it is worth remarking that the distribution shown later, as in Figure 8b, corresponds to the end of the transition when the temperature is much below 20 °C. In this case, a submicrometer average size is attained that is typical of this PIT emulsification process, but it is known that some variations are likely to happen depending on the temperature-change protocol.⁵⁵

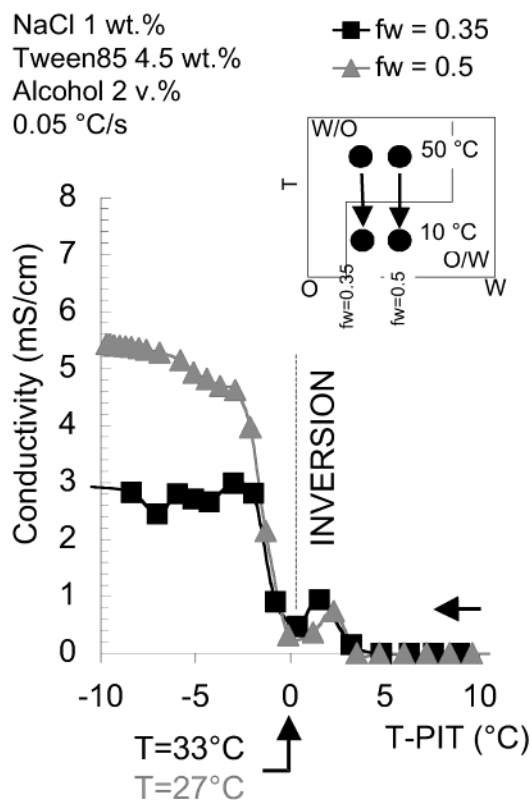


Figure 5. Conductivity variation versus temperature for two compositions.

The previously reported data corresponded to the case of a unit WOR, which is associated with the center of the formulation–composition map. Another composition with more oil content (FW = 0.35) is now selected to analyze the transition. It has been known for a long time³² that the WOR can alter the emulsion inversion temperature, in particular in the case of commercial ethoxylated surfactants that are mixtures in which the oligomers are likely to exhibit a selective partitioning between water and oil.⁵⁶

The diversity of the surfactant structure is probably aggravated by the fact that the ethoxylated sorbitan may be esterified up to four times. Consequently, the commercial product is probably a mixture of di-, tri-, and tetraesters. The general trend reported in partitioning studies is that an increase in the oil content tends to increase the selective partitioning of less hydrophilic species into oil, thus resulting in more hydrophilic species at the interface and, hence, in a shift of the three-phase behavior range toward a higher temperature. Figure 6 corroborates this trend because the PIT, taken as the start of the second rise in conductivity, is shifted from 27 °C to 33 °C as the FW decreases from 0.50 to 0.35.

Note that, in Figure 5, the temperature scale is taken as T_{PIT} , so that it is clearly seen that everything happens according to the same pattern, once the formulation scale is taken as a HLD equivalent. In both cases, the conductivity variation essentially exhibits the same features, along the $A^+ \rightarrow A^-$ transition, including the pre-inversion small bump in conductivity. The conductivity of the O/W emulsion is of course less in the FW = 0.35 case, and it seems that it reaches its plateau or normal O/W value much quicker.

(53) Salager, J. L.; Perez, M.; Garcia, Y. *Colloid Polym. Sci.* **1996**, *274*, 81.

(54) Salager, J. L.; Pérez-Sánchez, M.; García, Y. *Colloid Polym. Sci.* **1996**, *274*, 81.

(55) Miñana-Perez, M.; Gutron, C.; Zundel, C.; Anderez, J. M.; Salager, J. L. *J. Dispersion Sci. Technol.* **1999**, *20*, 893.

(56) Graciaa, A.; Lachaise, J.; Sayous, J. G.; Grenier, P.; Yiv, S.; Schechter, R. S.; Wade, W. H. *J. Colloid Interface Sci.* **1983**, *93*, 474.

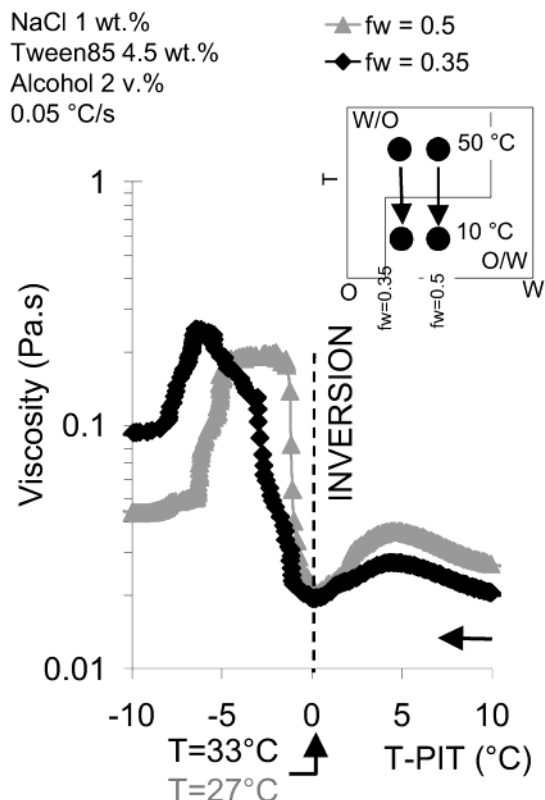


Figure 6. Viscosity variation versus temperature for two compositions.

This shift can be followed as well in the viscosity variation curves shown in Figure 6 in which the viscosity minimum coincidence with PIT produces a perfect match.^{57,58}

It is worth remarking that for $FW = 0.35$, the W/O emulsion (at $T > PIT$) has a lower internal phase ratio and is, thus, less viscous than the corresponding emulsion with $FW = 0.5$, whereas the opposite occurs for the w/O/W and O/W emulsions (at $T < PIT$). However, the viscosity of the 65% oil O/W emulsion is not much larger than the viscosity of the 50% oil O/W emulsion. The values clearly indicate that it is the 50% oil O/W emulsion that exhibits an anomalously high viscosity, and the only explanation is a w/O/W multiple morphology, with a lot of w inner droplets. Strangely enough, this means that the multiple emulsion is less likely to happen when there is more of the internal phase (oil). This should not be puzzling and is not necessarily general because the occurrence of multiple emulsions has been recently shown to depend on mechanisms and conditions that are far from intuitive.^{47,59–61}

The third case to be studied is on the right part of the map, where the system contains a large amount of water, that is, in the C zone. In this case ($FW = 0.7$), the transition takes place from C+ to C-, and the original emulsion is in the abnormal C+ zone and is, thus, likely to be a multiple emulsion of the w/O/W type.

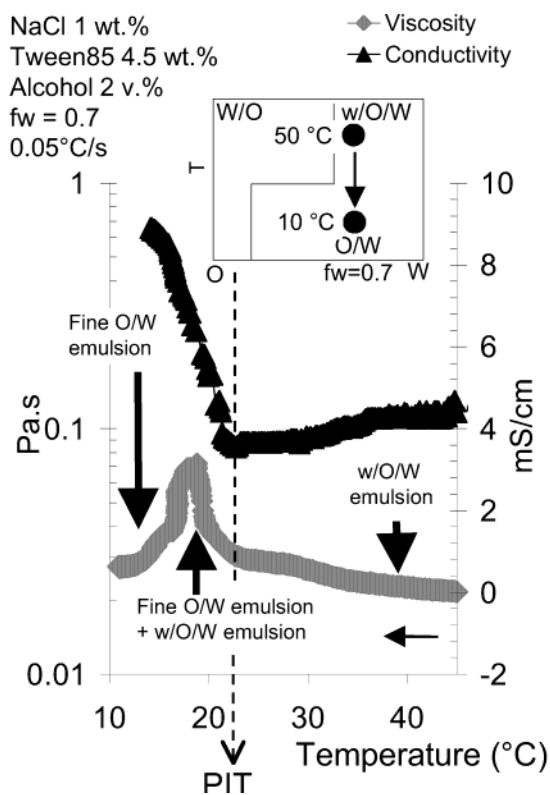


Figure 7. Viscosity and conductivity variations for $FW = 0.7$.

Figure 7 indicates the variations of the emulsion conductivity and viscosity when the temperature is decreased. In this experiment, the PIT value from phase behavior is slightly above 20 °C; it is lower than the one obtained at $FW = 0.5$. This result confirms that surfactant partitioning tends to shift the PIT to lower values when the oil content increases.

From 50 °C to 20 °C, the emulsion conductivity is high enough to denote a water external emulsion, of the w/O/W abnormal type with a percentage of encapsulated water droplets (w) of about 40–50% according to Bruggeman's law. After the three-phase behavior zone (20–18 °C) is passed through, the emulsion becomes a simple O/W type. However, the combination of conductivity and viscosity information tends to indicate that there is still a residual multiple emulsion w/O/W at the viscosity maximum. It is worth remarking that in this case there is no conductivity bump nor viscosity maximum at the temperature just above the PIT. Consequently, these features may be surely associated to the W/O morphology, which does not occur here at a temperature higher than the PIT.

For this experiment, it is easier to measure continuously the drop size because there is no change of the emulsion external phase. Figure 8a shows that at 48 °C, that is, essentially at the start of the experiment, the size distribution of the oil drops in the w/O/W emulsion is close to a log-normal curve with a $d(0.5)$ average at 26 μm . At 21 °C, the distribution becomes askew with tiny droplets smaller than 10 μm appearing, but there are still large drops, probably associated to the high emulsion instability associated to this region. It can be said that between 48 °C and 21 °C, oil drops containing tiny water droplets and simple fine oil droplets coexist. As the temperature decreases to attain the C- region, a submicrometric O/W emulsion is formed and saved according to the typical PIT protocol.

Figure 8b shows that the final drop distributions (at 10 °C) for the three experiments carried out at different WORs

(57) Sherman, P. *Encyclopedia of Emulsion Technology*; Marcel Dekker: New York, 1983; p 405.

(58) Pal, R.; Rhodes, E. *J. Rheol.* **1989**, *33*, 1021.

(59) Mira, I.; Zambrano, N.; Tyrode, E.; Márquez, L.; Peña, A. A.; Pizzino, A.; Salager, J. L. *Ind. Eng. Chem. Res.* **2003**, *42*, 57–61.

(60) Tyrode, E.; Mira, I.; Zambrano, N.; Márquez, L.; Rondon-Gonzalez, M.; Salager, J. L. Emulsion Catastrophic Inversion from Abnormal to Normal Morphology. 3. Conditions for Triggering the Dynamic Inversion and Application to Industrial Processes. *Ind. Eng. Chem. Res.* **2003**, *42*, 4311–4318.

(61) Zambrano, N.; Tyrode, E.; Mira, I.; Márquez, L.; Rodríguez, M. P.; Salager, J. L. *Ind. Eng. Chem. Res.* **2003**, *42*, 50–56.

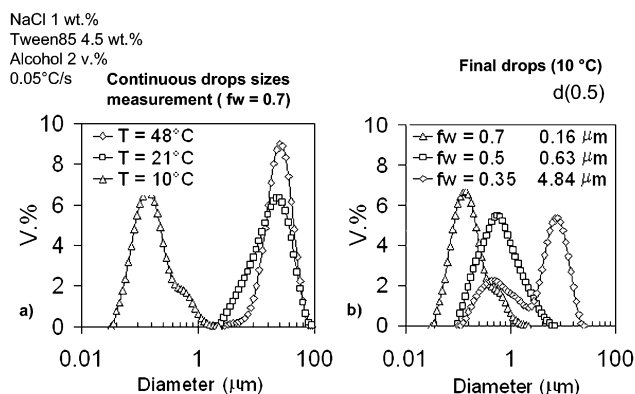


Figure 8. Drop size distribution in volume: (a) distribution at different temperatures for FW = 0.7; (b) final distributions at 10 °C for the three compositions FW = 0.7, 0.5, and 0.35.

are considerably different. The drop size increases as the FW is decreased. It is seen that a bimodal distribution, corroborated by microscopic observation, is exhibited for FW = 0.35, probably as a result of an uncomplete process with larger drops coming from the preinversion situation, and the small ones from the transition through a bicontinuous microemulsion structure.

In any case, it is obvious that the location of the PIT in the experimental range of temperatures (50→10 °C) has quite an influence on the final result, thus corroborating a previous study.⁵⁵

Conclusion

The simultaneous in situ measurement of both conductivity and viscosity has been carried out to monitor the dynamic transitional inversion from a W/O into a O/W emulsion as the temperature decreases. The complex morphologies exhibited around the inversion temperature can be elucidated more easily by the use of the dual conductivity/viscosity data. The existence of these complex morphologies is discussed as the result of the dynamic character of the transitional inversion process.

Acknowledgment. CONICIT-Venezuela and MAE-France are thanked for promoting the exchange of young researchers (J.A. and E.T.) through the Postgraduate Cooperation Program, PCP. The research carried out at Lab. FIRP has been sponsored by FONACIT (Agenda Petroleo 97-003719 and S1-2001-001156 Grants) and CDCHT-ULA.

LA035334R